

Optical Bistability in Fluorescein Dyes

S. Speiser* and F. L. Chisena

Allied-Signal Incorporated, Engineered Materials Sector P.O. Box 1087R,
Morristown, NJ 07960, USA

Received 30 September 1987/Accepted 26 November 1987

Abstract. Optical bistability has been observed in highly concentrated fluorescein dye solutions and in thin ($\sim 1 \mu\text{m}$) doped polymeric films. At concentrations larger than 10^{-5} mole/l dye dimers are formed. For fluorescein dye, the dimer-monomer equilibrium constant is 10^5 l/mole so that most of the dye species are in the dimer form. At 480 nm the dimer absorption cross section is 10^{-18} $\text{cm}^2/\text{molecule}$, while that for the dye monomer molecule is 7.6×10^{-17} $\text{cm}^2/\text{molecule}$. Upon laser excitation dimers dissociate to form monomers thus providing a highly nonlinear laser induced absorption. This high nonlinear absorption coefficient can be utilized for optically bistable response of the dye system.

Optical bistability was observed by placing dye solutions or dye thin films inside a Fabry-Perot resonator and exciting it with 480 nm dye laser pulses of 10 ns duration. The effect is more pronounced in 10^{-4} mole/l fluorescein than in 10^{-6} mole/l fluorescein in which dimer formation is not that efficient.

In disodium fluorescein no significant dimer formation is observed even at 10^{-3} mole/l dye concentration. The observed bistability both in solution and in thin films can be explained in terms of recent models for optical bistability in nonlinearly absorbing molecular systems.

PACS: 33, 42.65, 42.70

Optical bistability is by now a widely studied subject, mainly because of its potential use in optical data processors and optical computers [1, 2]. Optical bistability is characterized by two different light transmission states of an optical system for a given input light intensity [1, 2]. In order to observe optical bistability, a nonlinear optical medium and an optical feedback are required. As is the case with other nonlinear optical devices, good optical materials suitable for bistable devices are needed [3]. In recent years organic and polymer media have been investigated as potentially promising new optically nonlinear materials [4, 5]. The fluorescein dye was used as a nonlinear optical medium for a variety of applications [6, 7] which make this molecule a natural choice for optical bistability studies in nonlinearly absorbing media.

* On sabbatical leave. To whom correspondence should be addressed at Department of Chemistry, Technion-Israel Institute of Technology, Haifa 32000, Israel

In order to analyze optical bistability for various systems, we have developed [8, 9] the nonlinear complex eikonal approximation. Our goal was to set a standard mathematical treatment for the analysis of the propagation of light waves through nonlinear media. The lack of such a general treatment had complicated both the engineering modeling of optical systems incorporating nonlinear elements and better understanding of the related physical phenomena (since most of the other methods yield only numerical solutions for complicated cases).

The nonlinear eikonal approximation can be summarized in the following equation:

$$\phi(z) = (2\pi/\lambda_0) \int_0^z n[I(z')] dz', \quad (1)$$

where $\phi(z)$ is the complex accumulated phase, z the distance of propagation in the medium, n the nonlinear complex index of refraction, and $I(z)$ the local light intensity. This integral equation can be applied to

a variety of nonlinear media ($n(I)$) and to general schemes (or boundary conditions) ($I(z)$). We have demonstrated [8, 9] the applicability of the nonlinear eikonal approach for dispersive nonlinear resonators and we have obtained analytical results which were the first order approximation for the Fabry-Perot resonator case and the exact solution for the ring resonator. Recently we have extended the treatment to absorbing media [10] and in particular to molecular dye systems [11]. We were able to show that in addition to the obvious case of saturable-absorber optical bistability, one can expect to observe optical bistability due to excited singlet S_1 absorption [11]. Disodium fluorescein, discussed in the present paper, may be an example.

In many dye systems, however, complications due to dimer formation may destroy the desired nonlinear optical response. In this paper we treat such a system and demonstrate a novel type of optical bistability due to nonlinear absorption related to laser induced modification in the fluorescein monomer-dimer equilibrium.

1. Experimental

A Nd-YAG laser harmonic generated light (Quanta Ray DCR3) was used to excite a dye laser (Quanta Ray PDL-2). Dye laser light was used to excite dye solutions or dye polymer films placed in a Fabry-Perot resonator having mirror reflectivities of 90%. The input and output laser intensities are monitored by Hamamatsu 1188-06 PIN photodiodes and analyzed by a Tektronix 2430 digital oscilloscope interfaced to an IBM XT computer (Fig. 1a). Pump and probe experiments were performed using a 1% split off beam of the exciting laser, probing at an angle to the input beam (Fig. 1b). Laser induced fluorescence data were obtained by using a PTR monochromator and a Hamamatsu R928 photomultiplier (Fig. 1c). An Ophir 30-A-P laser energy meter was used to calibrate the photodiodes.

Thin films of up to 20 wt% of fluorescein in PMMA were prepared by dissolving the dye in trace ethanol and adding it to a solution (200 g/l) of PMMA (Aldrich, low molecular weight) in cyclohexanone. Films were spin coated onto fused silica substrates and dried at 80°C for one hour. The resulting thin films had a thickness of 1.5 μm and an absorbance of up to 0.7 at 480 nm.

2. Results and Discussion

Figure 2 shows the absorption spectrum of fluorescein at various concentrations. It is clear that Beer's law is

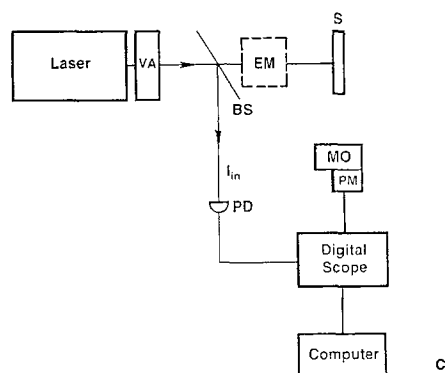
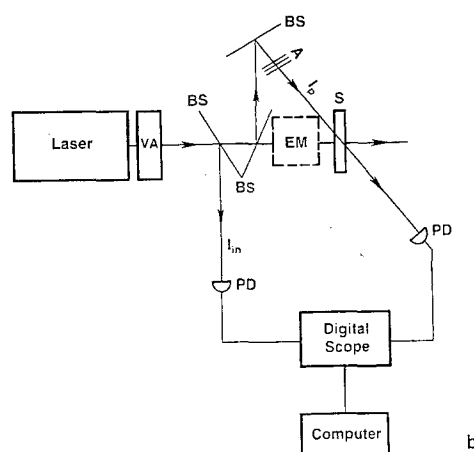
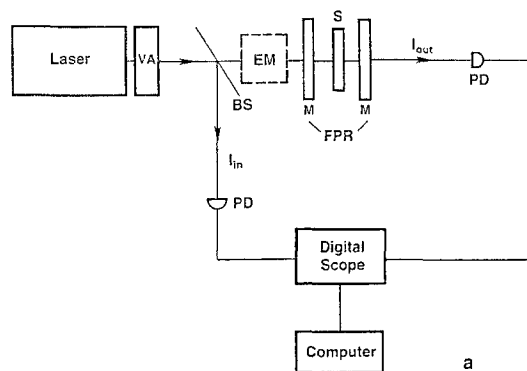


Fig. 1. (a) Schematic diagram of the experimental set up for measuring optical bistability; VA – variable attenuator, BS – beam splitter, PD – photodiode, EM – optional energy meter for calibration of the photodiodes, FPR – Fabry-Perot resonator, M – mirror, S – sample. (b) Set-up for laser induced absorption by the pump and probe method; A – attenuator. (c) Laser-induced fluorescence set-up; MO – monochromator, PM – photomultiplier

not obeyed, mainly because of dimer formation [12–14]. Similar spectra were obtained for fluorescein PMMA thin films. The following kinetic scheme can be used to describe the dimer(A_2)-monomer(A) equilibrium:



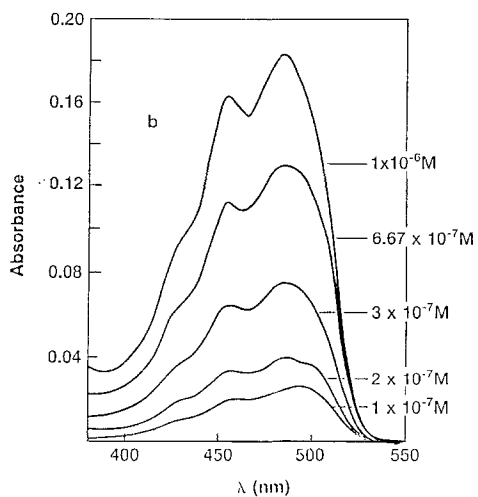
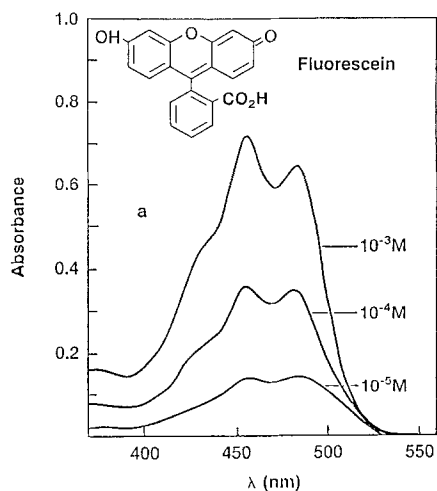


Fig. 2a, b. Absorption spectra for fluorescein solutions in ethanol (1 cm) path length (a) high concentration spectra (b) low concentration data

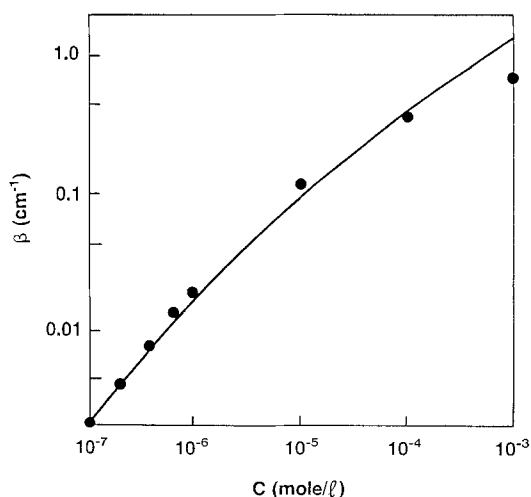


Fig. 3. Absorption coefficient β vs. concentration for fluorescein at 480 nm, the solid line is the best fit curve to (4)

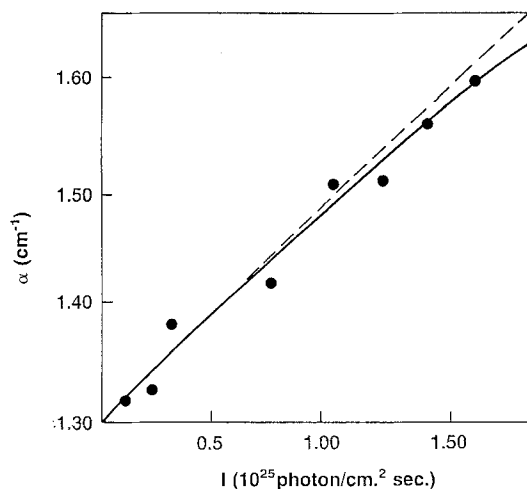


Fig. 4. Intensity dependent absorption coefficient, α for fluorescein 10^{-3} mole/l ethanol solution at 480 nm. The solid line is the best fit curve to (7), the linear fit is to (7a)

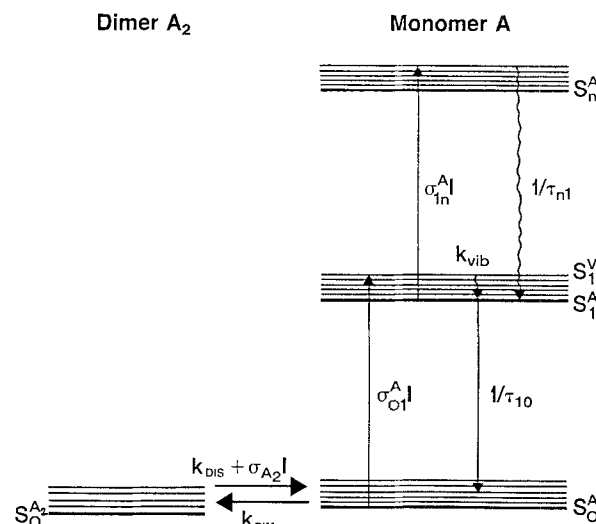


Fig. 5. Schematic energy level diagram for a dimer-monomer dye system. All rate processes are slow compared to the vibrational relaxation rate, k_{vib}

The effective absorption coefficient of the dye system is given by:

$$\beta = \epsilon_A(C - 2X) + \epsilon_{A_2}X, \quad (3)$$

where C is the total molar concentration, X is the equilibrium concentration of dimers, and ϵ_A and ϵ_{A_2} are the molar excitation coefficients of the monomer and dimer species, respectively. From a simple equilibrium stoichiometry we find

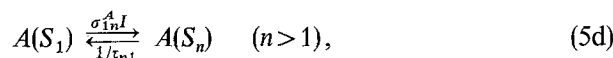
$$\beta = [(8KC + 1)^{1/2} + 1](\epsilon_A - \epsilon_{A_2}/2)/4K + C\epsilon_{A_2}/2, \quad (4)$$

where $K = k_{dim}/k_{dis}$ is the association equilibrium constant.

At low concentrations, Beer's law is observed yielding $\epsilon_A = 2 \times 10^4$ l/mole cm. Equation (4) can be

fitted to the β vs. C data of Fig. 2. The best fit curve is shown in Fig. 3 yielding $K=10^5$ l/mole and $\epsilon_{A_2}=260$ l/mole cm, the deviation at high concentration is probably due to the presence of higher aggregates.

Highly concentrated solutions of fluorescein which are highly dimerized might exhibit nonlinear absorption due to shift in the equilibrium of (2) towards monomer formation. This was examined by utilizing the laser pump and probe technique (at 480 nm). The absorption coefficient, $\alpha=2.3\beta$, as a function pump intensity, I , is shown in Fig. 4, exhibiting a marked nonlinear absorption. The increase in α as a function of pump intensity I can be analyzed by the following kinetic scheme of Fig. 5:



where S_0 , S_1 , and S_n denote ground, first excited, and higher excited singlet states respectively. Dimers are dissociated by laser pumping at a rate $\sigma_{A_2}I$, where σ_{A_2} is the dimer absorption cross-section. From the absorption data of Fig. 4, we calculate $\sigma_{A_2}=3.83 \times 10^{-21} \times \epsilon_{A_2}=10^{-18}$ cm²/mole. Monomers produced at a rate $\sigma_{A_2}I$ and are excited at a rate of $\sigma_{01}^A I$, where $\sigma_{01}^A=7.66 \times 10^{-17}$ cm²/mole is the monomer absorption cross-section, τ_{10} is the monomer fluorescence life time, and τ_{n1} is its S_n state lifetime [16].

Even for ns excitation, steady state conditions are reached [15] for fluorescein ($\tau_{10}=4.0$ ns [15]). Under these conditions, we obtain

$$K(I) = A_2/A^2 = k_{dim}/(k_{dis} + \sigma_{A_2}I) \\ = K/[1 + \sigma_{A_2}I/k_{dis}]. \quad (6)$$

This analysis is valid for pump intensities that are too low to induce any photoquenching of the monomer fluorescence due to excitation of $A(S_1)$ to higher singlet states at a rate $\sigma_{1n}^A I$ [σ_{1n}^A is the $S_1 \rightarrow S_n$ absorption cross-section, step (5d)] [15]. The intensity dependent absorption coefficient is thus calculated from Eq. (4) to be:

$$\alpha(I) = \{[8K(I)N + 1]^{1/2} + 1\} \\ \times (\sigma_{01}^A - \sigma_{A_2}/2)/4K(I) + N\sigma_{A_2}/2, \quad (7)$$

where N is the molecular concentration (molecule/cm³), $K(I)$ is in units of cm³/molecule, and I is in

units of photon/cm² s. At low intensities α approaches:

$$\alpha(I) = (\sigma_{01}^A - \sigma_{A_2}/2)[1 + 8KN]^{1/2} + 1 \\ \times (1 + \sigma_{A_2}I/k_{dis})/4K + N\sigma_{A_2}/2. \quad (7a)$$

This enhanced absorption should be manifested in basically two-photon induced fluorescence of monomers photoquenched at higher light intensities. Following standard photoquenching analysis [15] and neglecting contributions from step (5a) we find that the

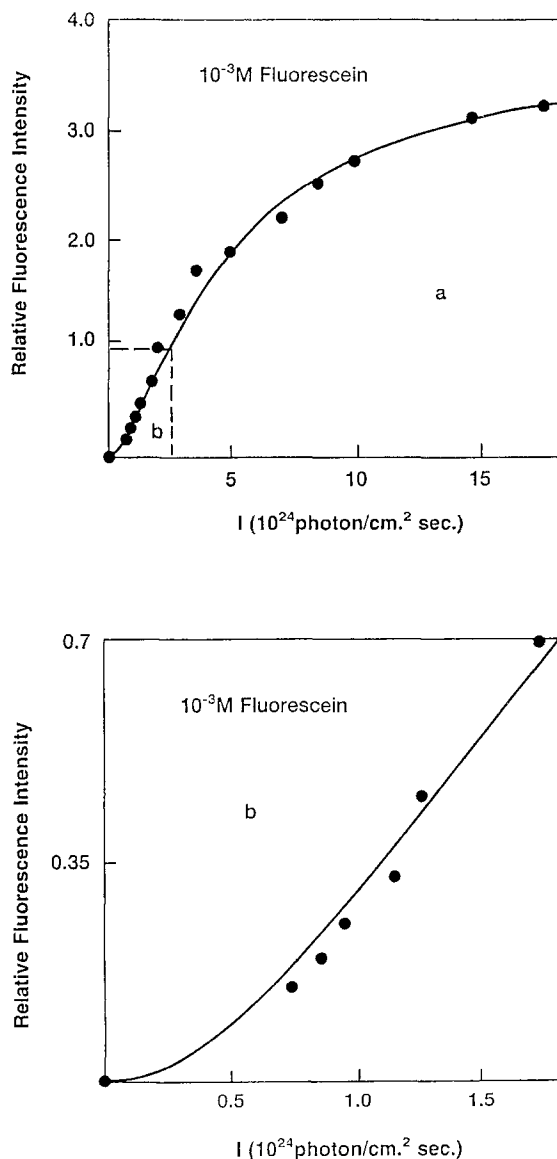


Fig. 6. (a) Laser induced fluorescence intensity for 10^{-3} mole/l fluorescein/ethanol solution 520 nm emission and (480 nm excitation). (b) A blow up of the $0-2 \times 10^{24}$ photon/cm² s region showing the quadratic dependence of the consecutive two-photon induced fluorescence resulting from dimer photolysis followed by monomer absorption. The solid line is the best fit to (8)

fluorescence intensity I_f is given by

$$I_f = \frac{\phi \sigma_{A_2} \sigma_{01}^A I^2 \tau_p}{1 + \tau_{10} \sigma_{01}^A I + \tau_{10} \sigma_{01}^A \tau_{n1} \sigma_{1n}^A I^2}, \quad (8)$$

where ϕ is the fluorescence quantum yield and τ_p is the laser pulse width.

Figure 6 shows a least square fit of (8) to 520 nm laser induced (480 nm excitation) fluorescence data for 10^{-3} mole/l fluorescein solutions. The value obtained from the best fit for $\tau_{10} \sigma_{01}^A$ is in good agreement with the calculated one. We may thus conclude that at these concentrations the fluorescein system is characterized by an absorption coefficient which is an increasing function of incident laser intensity. At 10^{-6} mole/l, fluorescein is mostly in the monomer form and laser induced fluorescence studies are typical of photo-

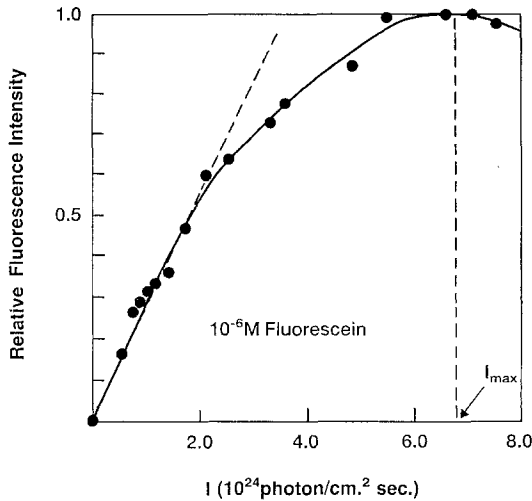


Fig. 7. Intensity dependence of laser induced fluorescence of 10^{-6} mole/l fluorescein (480 nm excitation)

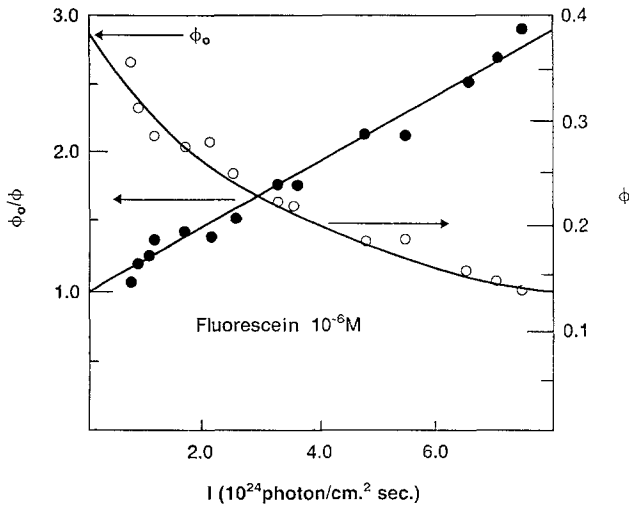


Fig. 8. Photoquenching plots [15] for 10^{-6} mole/l fluorescein

quenching process [15] for which

$$I_f = \frac{\phi \sigma_{01}^A I}{1 + \tau_{10} \sigma_{01}^A I + \tau_{10} \tau_{n1} \sigma_{01}^A \sigma_{1n}^A I^2}. \quad (9)$$

This behavior is exemplified in Fig. 7 for fluorescein monomers. The maximum I_f occurs at [15]

$$I_{\max} = (\tau_{10} \sigma_{01}^A \tau_{n1} \sigma_{1n}^A)^{-1/2}. \quad (10)$$

The reciprocal relative quantum yield is given by [15]

$$\phi_0/\phi = 1 + \tau_{10} \sigma_{1n}^A I, \quad (11)$$

where ϕ_0 is the limit of ϕ for $I \rightarrow 0$.

Figure 8 shows the fit of the experimental relative quantum yield to (11). For $\tau_{10} = 4$ ns we obtain that $\sigma_{1n}^A = 5 \times 10^{-17}$ cm²/mole, and $\tau_{n1} = 2 \times 10^{-10}$ s. Combining these results with the pump and probe experiment (Fig. 4) and using (7a), we obtain $k_{\text{dim}} = 1.6 \times 10^{13}$ l/mole s and $k_{\text{dis}} = 1.6 \times 10^8$ s⁻¹ [16].

Previous calculations have indicated that optical bistability should be observed in nonlinearly absorbing media [10, 11]. This prediction was tested here for the fluorescein dimer-monomer system. Figure 9b shows an increasing absorption optical bistability hysteresis loop obtained for this system at 480 nm. At low concentrations (10^{-6} mole/l) the loop disappears, as expected for solutions made of mainly monomer species, resulting in intensity independent α . It is clearly seen that the output pulse peaks before the input pulse due to increasing $\alpha(I)$. The slower decay of the output

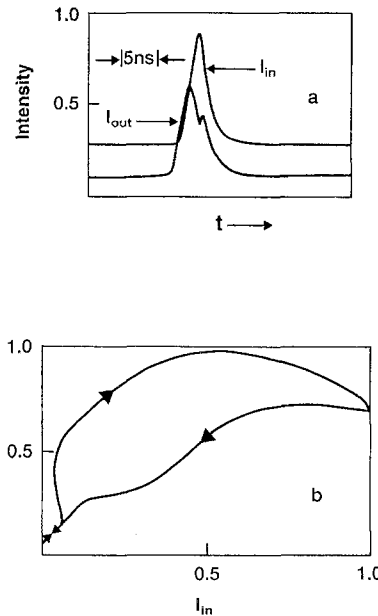


Fig. 9. (a) Input and output intensity 480 nm pulse for 10^{-3} mole/l ethanol solution of fluorescein in a Fabry-Perot cavity. (b) Optical bistability hysteresis loop for the dimer-monomer fluorescein system (480 nm excitation). Normalized scales

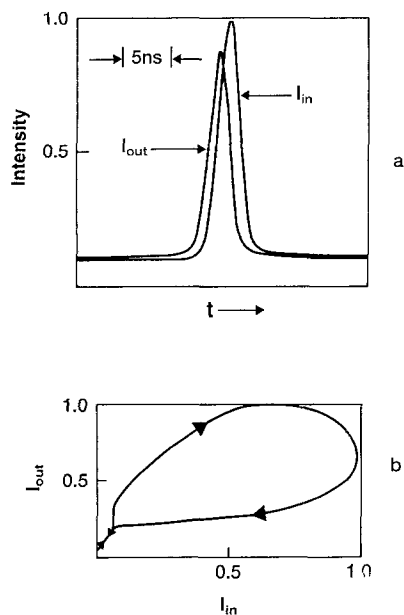


Fig. 10. Same as Fig. 9 for 2 μm thick fluorescein PMMA films ($\beta = 0.64 \text{ cm}^{-1}$)

pulse ($\sim 6 \text{ nsec}$, see Fig. 9a) reflects the recombination rate of monomers, which probably takes place within the solvent cage. It is satisfying to note that at 10^{-3} mole/l $k_{\text{dim}} \times C = 1.6 \times 10^{10} \text{ s}^{-1}$ corresponding to a decay time of 6 ns, thus supporting an in-cage recombination model [16].

For fluorescein doped PMMA thin films we observe similar bistable response (Fig. 10); however, the decay time of the output pulse is shorter probably due to faster monomer recombination in the more rigid polymer solvent cage.

Our conclusion, is that optical bistability can be observed in monomer-dimer dye systems. Such systems exhibit nonlinear absorption due to photolytic production of monomer species. In this respect it is a kind of photochromic system which was shown to exhibit optical bistability, [17], however, on a much longer time scale.

In order to observe optical bistability in a molecular absorber due to either absorption saturation or excited state absorption one has to look for systems free of higher molecular aggregates. Such a system is disodium fluorescein where dimer formation is known to be inefficient ($K = 5.0 \text{ l/mole}$) at the concentration range employed here [13].

The absorption spectrum of disodium fluorescein is shown in Fig. 11, no significant deviations from Beer's law are observed at concentrations lower than 10^{-3} mole/l , or in the PMMA doped thin film samples. Figure 12 shows a typical input and output 500 nm laser pulses for $9.45 \times 10^{-5} \text{ mole/l}$ disodium fluorescein ethanol solution together with the associated

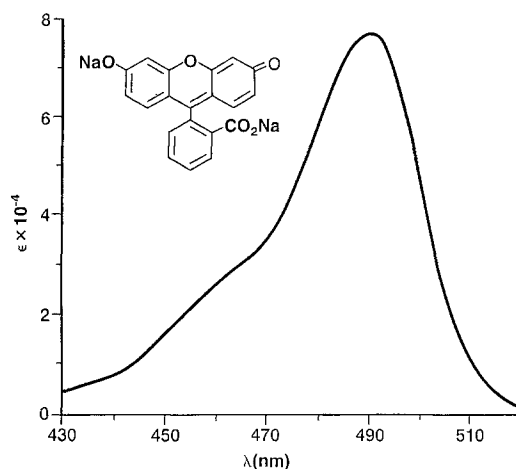


Fig. 11. Absorption spectrum for disodium fluorescein in ethanol solution. The same spectrum is observed in PMMA doped thin film

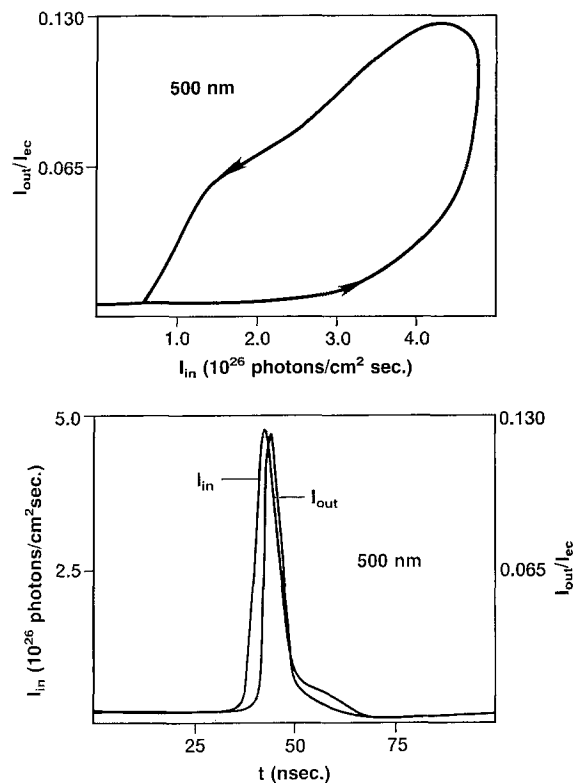


Fig. 12. Input and output intensity 500 nm pulses (bottom graphs) for 9.45×10^{-5} disodium fluorescein ethanol solution with the corresponding optical bistability hysteresis loop (upper graph)

optical bistability loop. The output intensity I_{out} is normalized to that of an empty cavity I_{ec} excited by the same laser input pulse (Fig. 13). It is evident that in this case optical bistability is characterized by a lag of the output pulse with respect to the input pulse and by an expected counterclockwise loop. The switching time of

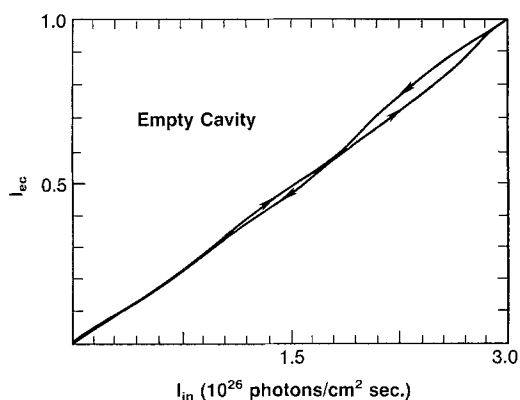


Fig. 13. Empty cavity response at 500 nm

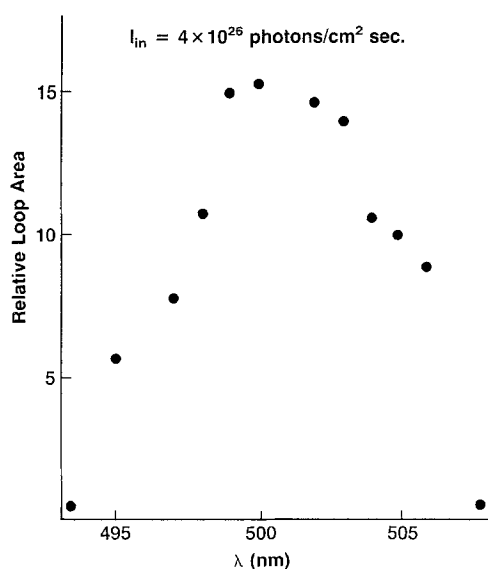


Fig. 14. Spectrum of the optical bistability area for disodium fluorescein

about 2 ns reflects the overall time response of the instrumentation rather than the actual switching time which is probably much shorter. The switching intensity is about 2.5×10^{26} photon/cm² s typical of laser intensities required for absorption saturation of singlet-singlet transitions in dye systems [15].

The optical bistability response of a molecular absorber is expected to depend on the optical density of the medium [11]. The best way to examine this dependence is by measuring the optical bistability spectrum. This can be done by simply measuring the area of the optical bistability loop as a function of the input laser frequency at a constant laser peak power and for a given sample concentration. The results for disodium fluorescein are shown in Fig. 14. Optical bistability is observed at a much narrow spectral range than that spanned by the absorption band. This result is in agreement with theoretical calculation of the

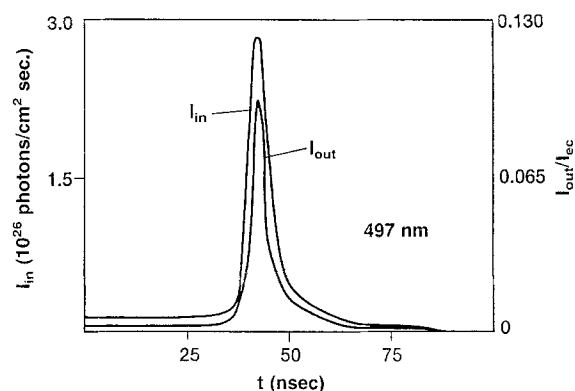
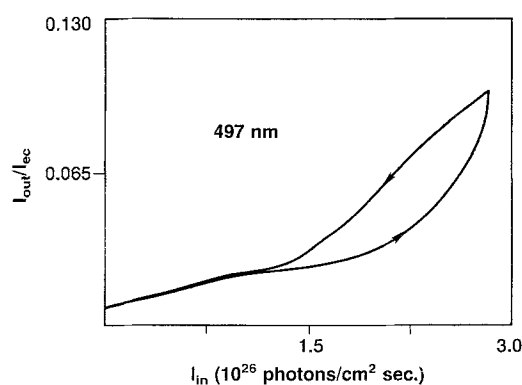


Fig. 15. Input and output intensity 497 nm pulses (bottom graphs) for 9.45×10^{-5} disodium fluorescein ethanol solution with the corresponding optical bistability hysteresis loop (upper graph)

spectral response of optical bistability of molecular absorbers [11]. Figure 15 shows the results of the optical bistability obtained at 497 nm. It exhibits some lag of the output pulse with respect to the input pulse with significantly smaller loop than that obtained at 500 nm (Fig. 14). Figure 16 shows results for 506 nm excitation. Here the output pulse proceeds the input pulse, resulting in a reversed bistability loop similar to that observed for fluorescein dimers (Fig. 9). Such a bistability loop is characteristic of intensity-induced increasing absorption [2]. This is to be expected as S_1 absorption for disodium fluorescein peaks at 530 nm and is more intense than S_0 absorption [15]. Thus excitation to the red of the absorption peak results in primarily S_1 absorption which increases with increasing pump intensity [15]. The fact that the bistability loop is reversed due to change in the electronic absorption mechanism suggests a purely electronic route for inducing optical bistability. This is the first example of purely increasing pump electronic absorption optical bistability. Samples of PMMA thin films doped with disodium fluorescein exhibit a similar response. It should be noted that this type of increasing absorption bistability is due to intensity induced

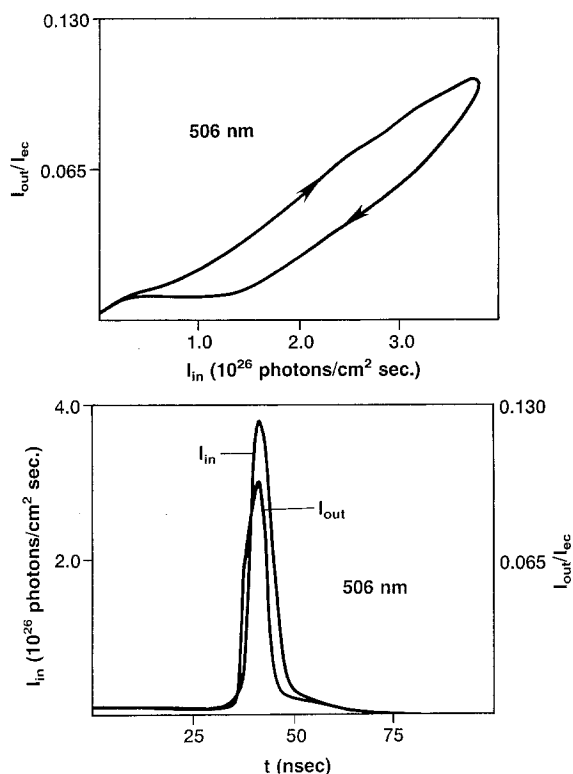


Fig. 16. Input and output intensity 506 nm pulses (bottom graph) for 9.45×10^{-5} disodium fluorescein ethanol solution with the corresponding optical bistability hysteresis loop (upper graph)

changes in the level populations and requires the resonator for feedback [10, 11]. This is a different situation compared to dynamically increasing absorption in semiconductors where cavity-less optical bistability is observed [20].

3. Conclusion

Our results on optical bistability in fluorescein show the suitability of dye systems for nonlinear optical applications. The optical nonlinearities involved are the same as those that determine fluorescein performance in four wave mixing and real time holography experiments [6, 7]. However, as was demonstrated here, depending on the conditions, fluorescein may dimerize and thus give rise to a novel type of optical nonlinearity [16]. For disodium fluorescein we have shown evidence for optical bistability due to either

absorption saturation or to excited state absorption, depending on the excitation wavelength. This is indicative of mainly electronic mechanism for inducing the bistability response, which is different from previous examples of optical bistability in dyes, which involve thermally induced nonlinearity [18, 19].

References

1. J.A. Goldstone: Optical bistability. In *Laser Handbook*, Vol. 4, M.L. Stitch, M. Bass (eds.) (North-Holland, Amsterdam 1985)
2. H.M. Gibbs: *Optical Bistability: Controlling Light with Light* (Academic, New York 1985)
3. A.R. Tanguay, Jr.: *Opt. Eng.* **24**, 2 (1985)
4. D.J. Williams (ed.): *Nonlinear Optical Properties of Organic Molecules and Polymeric Materials*, ACS Symposium Series 233, ACS, Washington, D.C., 1983
5. D.S. Chemla, J. Zyss: *Nonlinear Optical Properties of Organic Molecules and Crystals*, Vols. 1 and 2 (Academic, New York 1987)
6. T. Todorov, L. Nikolova, N. Tumova, V. Dragotinova: *Opt. Electron.* **13**, 209 (1981); *IEEE J. QE-22*, 1262 (1986)
7. M.A. Kramer, W.R. Tompkin, R.W. Boyd: *Phys. Rev. A* **34**, 2026 (1986)
8. M. Orenstein, S. Speiser, J. Katriel: *Opt. Commun.* **48**, 367 (1984)
9. M. Orenstein, S. Speiser, J. Katriel: *IEEE J. QE-21*, 1513 (1985)
10. M. Orenstein, J. Katriel, S. Speiser: *Phys. Rev. A* **35**, 1192 (1987)
11. M. Orenstein, J. Katriel, S. Speiser: *Phys. Rev. A* **35**, 2175 (1987)
12. R.W. Chambers, T. Kajiwara, D.R. Kearns: *J. Phys. Chem.* **78**, 380 (1974)
13. I. Lopez Arbeloa: Part 1, *J. Chem. Soc., Faraday Trans. 2* **77**, 1725; Part 2, *J. Chem. Soc., Faraday Trans. 2* **77**, 1735 (1981)
14. W.E. Ford: *J. Photochem.* **37**, 189 (1987)
15. S. Speiser, N. Shakkour: *Appl. Phys. B* **38**, 191 (1985) and references therein
16. Step (5b) may actually involve excitation to S_1 of A_2 followed by rapid dissociation, which is kinetically the same, see for example: S. Speiser, V.H. Houlding, J.T. Yardley: *Nonlinear optical properties of organic dye monomer-dimer-systems* (to be published in *Appl. Phys. B*)
17. C.J.G. Kirkby, R. Cush, I. Bennion: *Opt. Commun.* **56**, 288 (1985)
18. Z.F. Zhu, E.M. Garmire: *IEEE J. QE-19*, 1495 (1983)
19. M.C. Rushford, H.M. Gibbs, J.L. Jewell, N. Peyghambarian, D.A. Weinberger, C.F. Li: *Optical Bistability 2*, ed. by C.M. Bowden, S.L. McCall (Plenum, New York 1983) pp. 345-352
20. D.A.B. Miller: *J. Opt. Soc. Am. B* **1**, 857 (1984)